

MAGNETIC PROPERTIES RELY ON NUCLEATION AND GROWTH OF CORE-SHELL STRUCTURE NANOPARTICLES FORMED IN REVERSE MICELLE SOLUTION

GH. BAHMANROKH^{a,b}, M.B. HASHIM^b, S. BAWA^c, I. ISMAIL^b

^a*Department of Physics, Faculty of Science, Universiti Putra Malaysia, 43400 UPM, Serdang, Selangor, Malaysia.*

^b*Advanced Materials and Nanotechnology Laboratory, Institute of Advanced Technology, Universiti Putra Malaysia, 43400 UPM Serdang, Selangor, Malaysia.*

^c*King Fahd University of Petroleum and Minerals (HBCC campus), Harf Al-Baten, 31991, Kingdom of Saudi Arabia.*

This work is focused on the effect of reaction time on formation of nanoparticles by reversed micelles in the trimethylammonium bromide /*n*-octane/1-butanol extraction system. Adjusting the structural and morphological properties of the as-synthesized core-shell, cobalt-gold nanoparticles were highlighted and it is subsequently influences their magnetic properties. By employing controlled preparation conditions, the average crystalline size of the as-prepared samples was varied from 5 up to 20 nm. Configuration of single particles and clusters were reported by TEM and FESEM measurements. One of the significance of our work is to obtain high crystalline samples without applying any heat treatment. The degree of crystallinity of the as prepared samples was high like the ones after annealing. The room temperature magnetic measurements indicate that coercivity and remanence enhanced by increasing the particle size. Specifically, the as-prepared 8nm gold coated cobalt nanoparticles show very high coercivity, 1.175kOe, at room temperature. In addition the effect of annealing on structure and magnetic properties of Co-Au nanoparticles was studied.

(Received August 27, 2013; Accepted December 23, 2013)

Keywords: Coercivity, core-shell nanoparticle, Crystalline, Magnetic recording, Nucleation and growth, Reverse micelle

1. Introduction

In recent years, preparation and characterization of magnetic nanostructured materials are getting an immense importance to researchers. This group of smart materials is functional magnetic materials, where the magnetic properties decide their functional applications. Magnetic nanoparticles, amongst others, play an important role in biomedical applications, as carriers for targeted drug delivery within the human body or as heating agent for local hypothermic cancer treatment strategies [1]. Other potential applications envisage their use as building blocks for ultra-high density magnetic data storage media [2],[3] and for new generation of supercomputers.

Among the different magnetic nanoparticles studied to date, Co nanoparticles attract special attention as a consequence of specific behaviors. People have synthesized Co-CoO core-shell type, nanoparticles of 8nm fcc cobalt core with 2nm shell fcc CoO [4], Co-Si core-shell nanoparticles [5] and cobalt-coated gold nanocrystals [6], [7]. Investigation the effect of coating of cobalt nanoparticles with various metals and oxides have been a remarkable area for researchers.

*Corresponding author: ghazalehbahmanrokh@yahoo.com

Also the possibility of preparing nanosized metal particles with homogeneous morphology and size is of great interest because such particles have extremely small size and large specific surface area. Additionally, the shape control of nanoparticles is recognized as a very important issue in the nanoparticle synthesis, which became a challenging task [8], [9].

Various methods have been widely used for the synthesis of nanosized cobalt with different shapes and morphology. The co-precipitation and sol-gel method are used to prepare metal oxide or composite metal oxide by chemical reaction [10], [11]. Thermal decomposition of organic compounds in an organic media is also an available method for preparing inorganic material. But these methods are mostly performed under a certain temperature and pressure, that is to say, an operation condition is somewhat critical [12] [13]. Proposing a convenient way for synthesis nanomaterials have been a challenge for researchers during last decades.

Alternative method of micellar technique is a good candidate for the synthesis to control the particle size in nano regime. Some advantages of micellar over other techniques are soft chemistry, demanding no extreme pressure or temperature control, and requiring no special or expensive equipment. It is well known that surfactant form the micelles above certain concentration. Reverse micelles are generally described as nanometer-sized water droplets dispersed in a polar solvent. Surfactant forms a monolayer at the interface between the oil and water. Due to dynamic character of micelles, the reactants come into contact with micelles, which subsequently results to the nucleation and growth of metal particles upon reduction occurs inside the water pools. Micelles house the particles, thereby restricting its size in nano regime. Micelles are used not only to control the size; the shape of the particles can also be controlled. The aim of this paper is to prepare cobalt nanoparticles coated with gold with different dimensions by controlling the size of reversed micelles by changing the molar ratio of water to surfactant. In addition varying the time of stirring caused to get both clusters and single particles. The effect of time on structure and magnetic properties of clusters and single particles is of our interest in this paper. The morphology, structure and magnetic properties of these particles analyzed and subsequently reported.

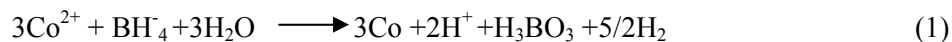
2. Experimental

1) Materials

For the synthesis of Co-Au nanoparticles, the following commercial reagents were used; $\text{Co}(\text{NO}_3)_2 \cdot 6\text{H}_2\text{O}$ (ACRÖS organics , 98%), AuCl_3 (Alfa Aesar, 99%) as metal basis, NaBH_4 (ACRÖS organics , 99%) as reduction agent, trimethylammonium bromide (CTAB) (R&M chemical, 99%) as cationic surfactant, 1-butanol (Sigma Aldrich, 99.8%) as co-surfactant and n-octane (ACRÖS organics , 99%) as the oil phase. Deionized water was used throughout the experiment. Besides, chloroform and methanol were used as washing agents.

2) Preparation of nanoparticles

The experiment was done under argon atmosphere to prevent oxidation. Four appropriate rations of aqueous phases containing 2 metal salts and 2 reducing agents were prepared. The mixed reverse micellar solutions containing aqueous phase were injected into an n-octane solution of CTAB and 1-butanol. Each solution stirred magnetically to get the clear and optically transparent solution. Reverse micelle containing sodium borohydride was slowly added to reverse micelle of cobalt salt under stirring. The color of solution was changed from light pink to black during nucleation process. At that stage, black precipitations in solution was evident. The micellar solution containing Au aqueous solution was continuously added to the resulting solution, which cause coating the cobalt nanoparticles followed by reduction of Au^{3+} to Au. The experimental procedure is described by the following equations:



After stirring the final solution at room temperature in different times, the resulting particles were separated using centrifuge at 3500 rpm. The surfactant was finally removed by successive washing with chloroform/methanol (1:1) and then dried at room temperature. Parts of solids were annealed at 400 °C for 2 hours under argon.

3) Characterization

X-ray diffraction (XRD) measurement were performed by Philips X-ray diffractometer (model 7602 EA Almelo) at a scanning rate of 5°/min in the 2θ range of 20° to 80°, using a monochromatized CuK α radiation ($\lambda=1.5418$ Å). The microstructure studies were performed using transmission electron microscopy (TEM) (Hitachi -7100) with an accelerating voltage of 120 kV and field emission scanning microscopy (FESEM). Samples for these measurements were prepared by depositing a drop of the dispersion in the solvent of ethanol onto carbon-coated copper grids and the grids were dried in air. The magnetic measurement was carried out using vibrating sample magnetometer (VSM) (model Lakeshore, 7404 series) at room temperature. Hysteresis measurements were performed with maximum applied magnetic field of 2T.

3. Results and discussions

Micelle is an aggregate of surfactant molecules dispersed in a liquid colloid. A typical reverse micelle in aqueous solution forms an aggregate with hydrophobic single tail regions in contact with surrounding solvent, sequestering the hydrophilic "head" regions in the micelle centre. The TEM images of the initial solution that contains micellar media were taken to certify the formation of these micelles or water droplets in oil, as shown in Figure 1. The images show precipitations in the water droplets covered with surfactant and co-surfactant molecules in the oil phase. The images were taken after two weeks, leaving the grids to dry at room temperature. From the images we can see the aggregates of 20-60 nanoparticles surrounded with surfactant molecules. The average size of each cluster was approximately 200 nm. Figure 1b shows the clusters at higher magnification. In contrast, Figure 1c illustrates a single nanoparticle. These suggest the formation of two kinds of structures; one with single nanoparticles and the other, a collection of smaller or single nanocrystals in clusters.

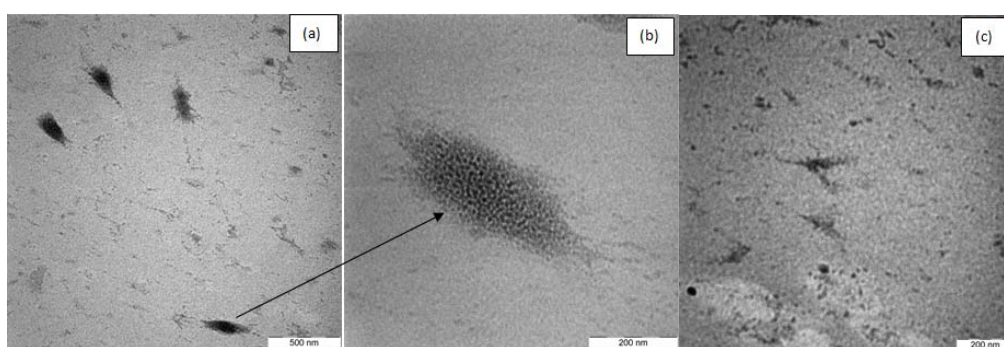


Fig. 1. TEM image of surface passivated Co-Au nanoparticles with CTAB and 1-butanol

Other measurements were performed on particles after washing. XRD diffraction results for Cobalt-gold nanoparticles before and after annealing at 400°C referred to 4 different ω : 5, 10, 15, 20 are shown in Fig. 2 a and b respectively. According the gold coverage, most mean peaks at 38°, 44°, 64° and 77° matched with cubic Au with (111), (200), (220) and (311) plans of crystals and 44°, 51° related to cubic cobalt. No peak was observed for cobalt oxide due to gold coating. Figure 2b demonstrates that annealing did not influence the peaks position. There was no

significant change observed for crystal lattice (4.07\AA with $d_{111} = 2.35^\circ$) and the volume cell (67.90\AA^3) for the main diffraction peak before and after annealing for different ω ratios. For all samples before and after annealing the major peak ($2\theta = 38^\circ$) was used for crystal size measurement by Scherer formula.

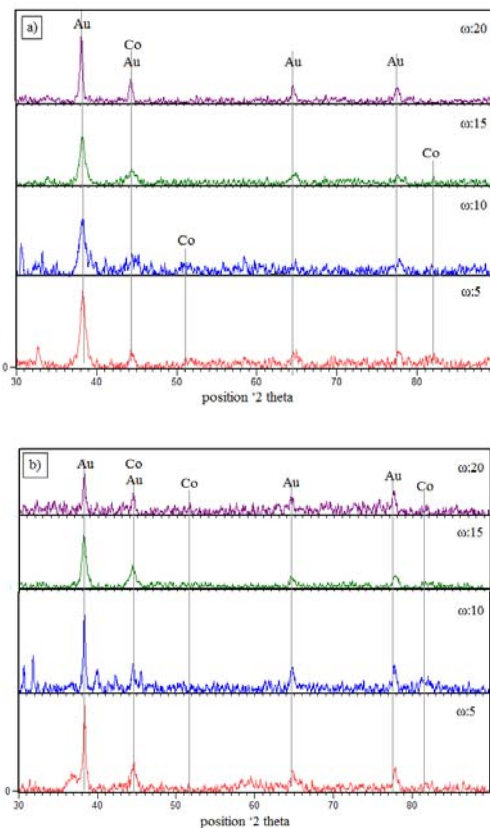


Fig 2. XRD plots of a) Co-Au as prepared. b) Co-Au after annealing in 400°C for 2 hours.

Comparing plots for different ω , shows that the peak broadening is purely due to the reduction of ω . Relation between Full Width at Half Maximum and ω for samples before and after annealing is shown in Figure 3. The increasing in FWHM is related to reduction in particles size which is proportional to the molar ratio of water to surfactant. Also it indicates that after annealing FWHM has lower value than as prepared. This trend is consistent with the widely accepted phenomena.

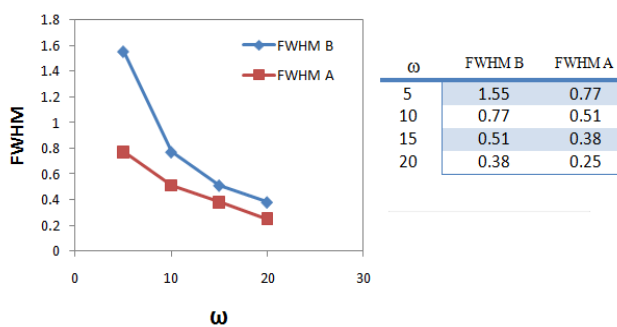


Fig. 3. FWHM B: Full Width at Half Maximum before annealing, FWHM A: after annealing. ω : $[\text{H}_2\text{O}]/[\text{CTAB}]$

The morphologies and size distribution of the as prepared samples were examined using TEM analysis. The result shown in Figure 4 revealed the TEM images of products obtained at different concentrations (ω : 5, 10, 15, 20). The figures illustrate that a decrease in CTAB concentration is correlated to increase in diameter of particle size. The size distribution notify even most particles are in 5, 10, 15 and 20 nm but the average size is bigger and are 8.3, 13.3, 25.6 and 21.34 respectively. The black and gray particle colors in figure 4b specify core-shell structure of cobalt and gold.

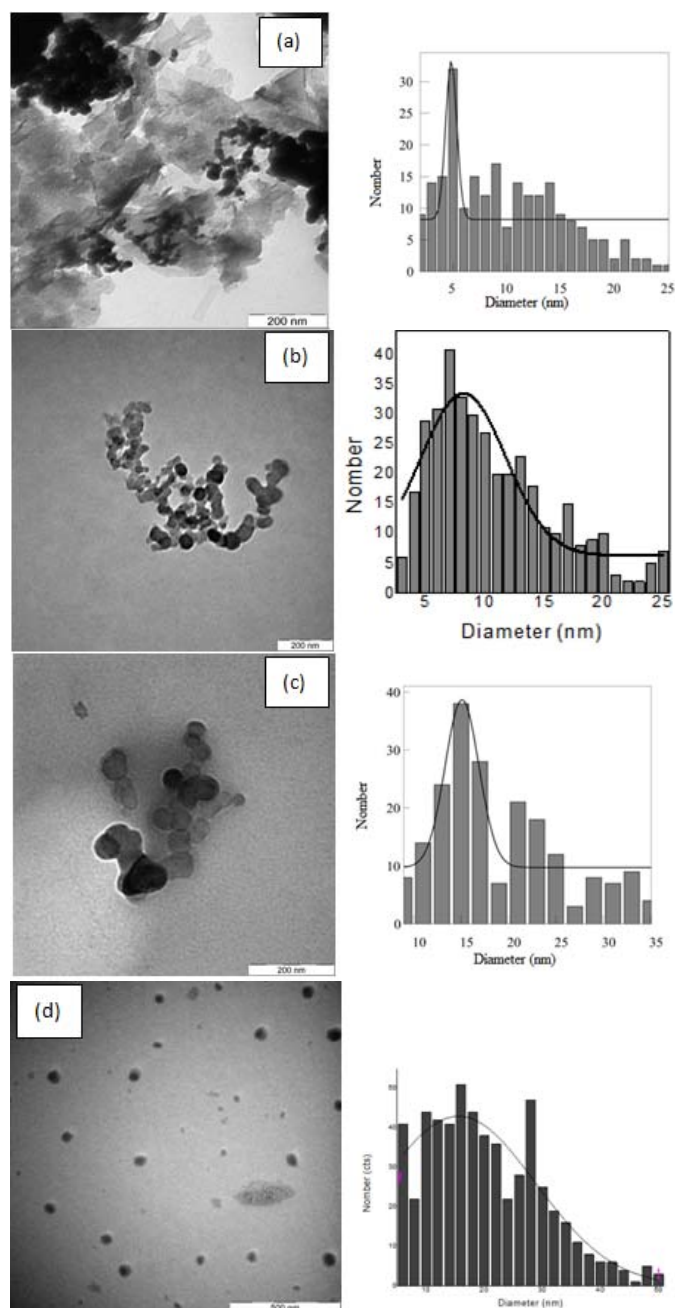


Fig.4. a, b, c, d are TEM images for samples with ω : 5, 10, 15, 20 respectively and their size distributions.

Table 1 compares the average particle size measured over 200 particles by TEM, and the XRD crystal size calculated by Scherrer formula;

$$D_p = \frac{k \lambda}{\beta_{1/2} \cos \Theta}$$

where D_p is the crystallite size, λ the wavelength of the x-ray radiation, K is the shape factor which has different values varies with the actual shape of crystallite, and β is the line width at half maximum height. From the table, a slight change was observed between the average particle size obtained by TEM and crystalline size obtained by XRD. This is attributed to be normal since the crystalline size is smaller than the particle size. Figure 5 shows a graph summary of the results in Table 1. As we can see from figure 5 with increasing in ω values, both crystal and particle size increases.

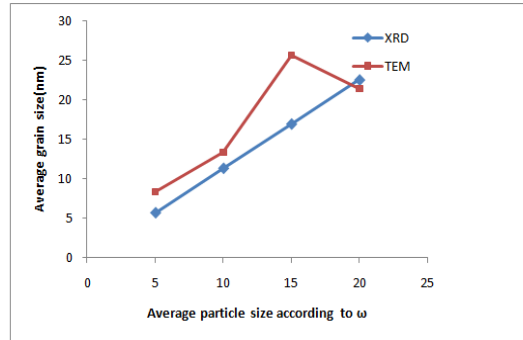


Fig.5. The mean particle size from TEM and XRD compared with ω for as prepared samples.

Table 1. Summery of crystal size and mean size of particles for ω : 5,10, 15, 20.

ω	crystallite size(nm) XRD (B)	particle size(nm) TEM (B)	crystallite size(nm) XRD (A)	particle size(nm) TEM (A)
5	5.6	8.3	11.4	-
10	11.2	13.3	17.2	21.6
15	16.9	25.6	23.1	-
20	22.5	21.3	35.1	34.2

FESEM studies showed the formation of cloudy appearance for ω :5 in 10k magnification however change the mode from secondary electrons to back scattered cause shiny dots appears indicating gold shells on cobalt surface demonstrating that particles are inside clusters. At higher magnification formation of arrays of small shiny dots was detected. The average size of each cluster was reported 259 nm. In Figure 6c, d, e we can see increasing the clusters size with increasing the average sizes in the nanometer range of 259, 339,380nm for ω : 5, 15 and 20 respectively.

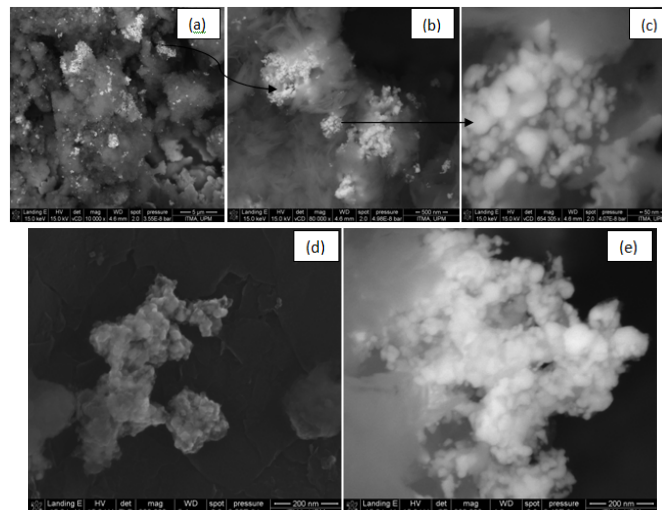


Fig. 6. a, b, c FESEM image of sample ω : 5 with increase in magnification. d, e for ω : 15, 20

Figure 7 shows magnetization curve over magnetic field at room temperature for samples before and after annealing. All four samples with different ω ratios 5, 10, 15, 20 nm represent single-domain behavior and were soft as prepared and particularly in between superparamagnetic and paramagnetic behavior. However the single-domain particles show paramagnetic and superparamagnetic behavior but some coercivity was reported from VSM measurements indicating the interaction between moments and existence of coupling energy which is a character of single domain ferromagnetic materials. Superparamagnetic materials have zero coercivity which is the character of these materials. From the VSM results significantly high coercivity was recorded which is due to ferromagnetic behavior of the samples. We can declare that our samples are single-domain ferromagnetic while their size is below critical size[14]. These samples exhibited strong annealing effects, and the coercivity increased after annealing in 400°C for 2h. The coercivity for smaller samples were significantly larger than the coercivity consistent with size measurements that show a predominance of larger grains [15]. Figure 9a indicates that the coercivity for as synthesized samples increases once the particles size decreases. Saturation magnetization decreases slightly with increase the particle size but significantly increases to 7emu/g with increase the grain size to 25.6nm, which is consistent with the established phenomena. Table 2 summarizes magnetic properties for samples before and after annealing. The increase in coercivity and saturation magnetization after annealing was evident. This variation is also explained on the basics of domain structure, diameter of particles and crystal anisotropy[16].

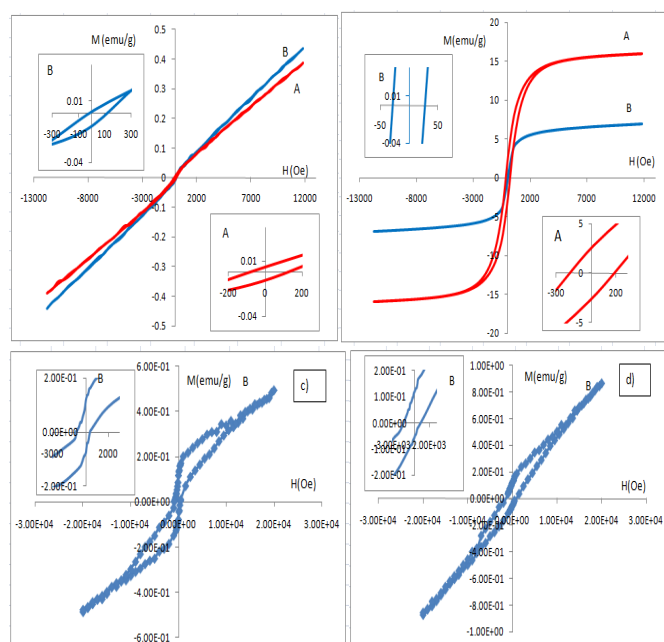


Fig. 7. Magnetization (M) curve over magnetic field at room temperature, a) ω :20, b) ω :15, c) ω :10, d) ω :5. A: after annealing and B: before annealing.

Table. 2. Magnetic properties of cobalt-gold NPs under different states before and after annealing.

Sample Co/Au	ω	grain size TEM	H_d (Oe)	M_s (emu/g)	M_r/M_s	H_c (Oe)	μ_{grain} (emu/Oe) $\times 10^{-7}$
as prepared	5	8.3	1175	0.8	0.1	18507	9.39
annealed	-	-	337	0.85	0.11	19994	18.9
as prepared	10	13.3	639	0.25	0.2	18542	31.4
annealed	-	21.6	1066	0.5	0.5	19976	9.14
as prepared	15	25.3	27	7	0.033	-	-
annealed	-	-	187	16	0.160	-	-
as prepared	20	21.3	63	0.38	0.012	-	-
annealed	-	34.2	99	0.43	0.015	-	-

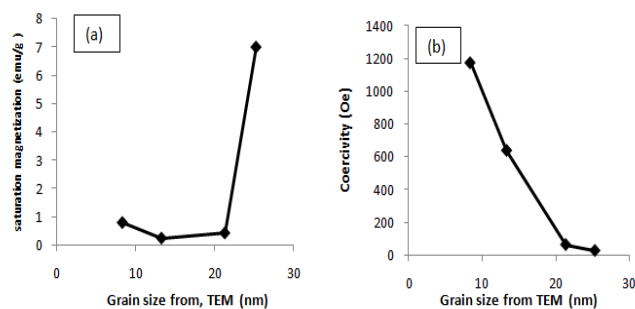


Fig. 8. a) Saturation magnetization over grain size and b) Coercivity over grain size for samples before annealing.

Table 3. Dependence of time to the average particle size by TEM and ω .

ω : [H ₂ O]/[CTAB]	Mean particle size by TEM (nm)	Time of total reaction (min)	Morphology
5	8.3	60	Clusters and spherical Nps
10	13.3	20	Clusters and spherical Nps
15	25.6	120	spherical Nps
20	21.3	120	spherical Nps

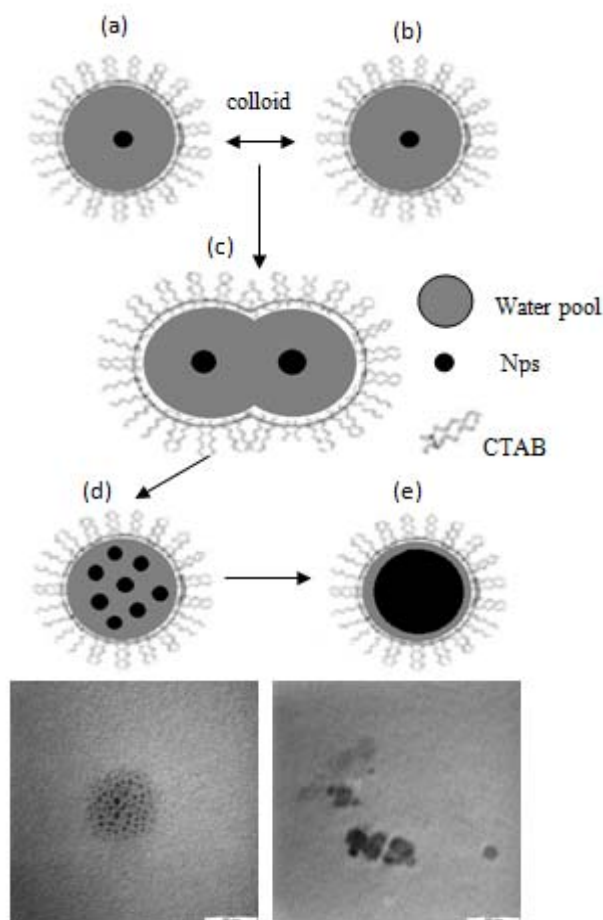


Fig 9. Formation of cobalt precipitation in water pools of 10nm. a ,b) one single nano cobalt crystal. c) coalescence and colloid process of a and b. d) some small nanocrystal encapsulate in one water droplet. e) agglomeration of small nanocrystals. TEM images for sample ω :10.

In detail the squareness of the loop increases after annealing in all cases. According to Figure 8 the room temperature coercivity of the Co-Au magnets increases with decreasing grain size. A small grain size is advantageous to reduce surface degradation[17].

The coercivity of magnets is determined by the magnetocrystalline field strength, reduced by local demagnetizing fields. The local fields depend on the volume and the shape of the reversed grains. Hence in magnets with a reduced grain sizes the local fields and the probability of the nucleation of reversed domains will be smaller, that results in increased coercivity, see Table 2.

In microemulsions method precipitation occur due to the collision and coalescence of droplets in continues phase. At the beginning of the reaction and reduction process only one single nanocrystal exists in water droplet (see stage a and b in Figure 9) but during collision process and van der waals attraction between the droplets may exist more than one nanoparticle due to double layer structure that appears on the surface of an object when placed into a liquid (stage c in Figure 9).

It is reported that increase the time or temperature of reaction cause growth of bigger particles [18]. This informed the conduct of this experiment at room temperature with no heat treatment during synthesis. From the results of TEM image we have seen formation of more clusters instead of single particles for ω : 10 to compare with ω : 15 and 20. The reason is the decrease in time of reaction to 20 min, enough time for nucleation but not for growth. The time dependent morphology of particles is summarized in table 3. Reduction process with NaBH_4 is very fast and is an exothermic followed by release of H_2 gas during nucleation. After reduction the extra stirring time is cause to growth of nanoparticles. The two droplets enclose cobalt salts will collide and cause to existence of more than one single nanocrystal in singlr water droplet is shown in Figure 9d. With increase the time some of these nanocrystals will agglomerate and results bigger particles at Figure 9e. The molar ratio of water to surfactant controls the water pools by re-separate and return back to its original size. The schematic of the process is outlined in Figure 9. Comparing the time and the mean particle size by TEM in table 3 shows that while the reaction time remains constant for ω : 15, 20 but the mean size for ω :15 was higher than ω :20 , 25.6 and 21.3 respectively. This indicates that agglomeration happens in smaller particles more than the bigger ones and cause formation of bigger particles during the reaction time.

3. Conclusion

In this paper we have prepared cobalt nanoparticles coated with gold in reverse micelle solution.

During nucleation and particle growth by Brownian motion and colloidal process, two kind of formation processes were observed; small single crystalline and bigger particles. Bigger particles are formed due to agglomeration of smaller particles together in solution by increasing the time of stirring.

The structure of mixed reverse micelles is mainly utilized as a template to limit the crystal nucleation and growth. Crystal size calculated by Scherer formula and average grain size measurement via TEM were in good agreement with ω (the molar ratio of water to surfactant).

All as synthesis samples were highly crystalline without applying any heat treatment during synthesis using reverse micellar technique.

The sample with ω :5 shows very high coercivity at room temperature before and after annealing and has low saturation magnetization due to its very small grain size.

Acknowledgment

The authors are grateful to I. Ismail who carried out the FESEM images and we would like to thank E. Othman (Advanced materials research centre, SIRIM BERHAD) for VSM, measurements.

References

- [1] Q. Pankhurst, et al., *Journal of Physics D: Applied Physics*, **36**, R167 (2003).
- [2] S. Sun, et al., *Science*, **287**, 1989 (2000)
- [3] S. Sun, *Advanced Materials*, **18**, 393 (2006).
- [4] M. Spasova, et al., *Journal of Magnetism and Magnetic Materials*, **272-276**, 1508 (2004).
- [5] W. Fu, et al., *Materials Chemistry and Physics*, **100**, 246 (2006).
- [6] Y. Bao, K. M. Krishnan, *Journal of Magnetism and Magnetic Materials*, **293**, 15 (2005).
- [7] G. Cheng, A. R. Hight Walker, *Journal of Magnetism and Magnetic Materials* **311**, 31 (2007)
- [8] K. Brown, D. Walter and M. Natan, *Chem. Mater*, **12**, 306 (2000).
- [9] D. Chen, et al., *Journal of Alloys and Compounds*, **475**, 494 (2009).
- [10] B. Niemann, et al., *Chemical Engineering and Processing*, **45**, 917 (2006)
- [11] Z. Li, et al., *Journal of Central South University of Technology*, **7**, 57 (2000).
- [12] C. L. Dennis, et al., *Magnetics, IEEE Transactions on*, **43**, 2448 (2007)
- [13] M. Salavati-Niasari, Z. Fereshteh, F. Davar, *Polyhedron*, **28**, 1065 (2009).
- [14] M. Sato and Y. Ishii, *Journal of Applied Physics*, **54**, 1018 (1983).
- [15] W. Rodewald, M. Katter and K. Uestuener, 2004, pp. 486.
- [16] S. B. Waje, et al., *Journal of Magnetism and Magnetic Materials*, vol. 322, pp. 686-691.
- [17] M. Rajendran, et al., " *Journal of Magnetism and Magnetic Materials*, **232**, 71 (2001).
- [18] J. Penuelas, et al., *Surface Science*, **602**, 545 (2008).